Application of High-Pressure Electron Paramagnetic Resonance (EPR) Spectroscopy in Protein Science

Austin MacRae, [1,#] Zoe Armstrong,[1,#] Mary Lenertz, [1] Qiaobin Li, [1] Aiden Forge, [2] Max Wang, [3] Li Feng, [1] Wenfang Sun, [4] Zhongyu Yang[1,*]

1. Department of Chemistry and Biochemistry, North Dakota State University, Fargo, North Dakota 58102

2. Dilworth Glyndon Felton High School, Dilworth, Minnesota 56547

3. California State University San Marcos, San Marcos, California 92096

4. Department of Chemistry and Biochemistry, University of Alabama, Tuscaloosa, AL 35487

Corresponding to: zhongyu.yang@ndsu.edu

# these authors contribute equally

Abstract

High hydrostatic pressure at a few thousand bars has been found to offer an opportunity to probe protein conformational states which possess lower hydrostatic volumes and are often not well-populated under the ambient pressure. An important contribution of Prof. Wayne Hubbell is to initiate EPR studies on proteins under elevated pressure via establishing the theoretical basis of high pressure EPR so that parameters from EPR measurements can be corelated to key protein structural factors such as activation volume and molar compressibility. Prof. Hubbell also developed a series of experimental devices for the measurement of continuous wave (CW) and double electron-electron resonance (DEER) EPR under elevated pressure. These efforts have directly resulted in a series of high pressure EPR studies on globular and transmembrane proteins. Via this review in the current Special Issue, we aim to briefly cover the most recent findings in high-pressure EPR and its applications in protein science. We will focus on what each technique can do in protein studies, how to use the technique to measure needed information, and what each measured parameter tells us. We will also discuss the combination of high-pressure EPR with other techniques and the future perspectives of the field. The ultimate goal is to broaden the application of high pressure EPR and its combination with other high pressure biophysical techniques to improve protein science research.

1. Introduction

High hydrostatic pressure is a key physical chemistry parameter and has been known to play important roles in nature, from as large as organisms to as small as proteins. Pressure at the scale of a few thousand bars is of particular interest to protein science because it offers an opportunity to probe protein conformational states which possess lower hydrostatic volumes and are often not well-populated under the ambient pressure, following the La Chatelier's principle. For two protein conformational states in equilibrium, the pressure dependence of the equilibrium constant K is given by:[1, 2]

$$\ln\left(\frac{K(P)}{K(0)}\right) = -\frac{\Delta\bar{V}^0}{RT}(P) + \frac{\Delta\bar{\beta}_T}{2RT}(P)^2 \qquad \textbf{[1]}$$

Where R is the Boltzmann constant, T is temperature in Kelvin, P is the pressure, V is volume, K(P) and K(0) are the equilibrium constant K at P and 0 bar pressure, respectively, $\Delta\bar{V}^0$ is the difference in partial molar volume of the two conformational states, and $\Delta\bar{\beta}_T$ is the difference in partial molar isothermal compressibility of the two conformational states in respect to the standard condition (1 bar and 294 K). $\Delta\bar{\beta}_T$ is defined as

$$\Delta\bar{\beta}_T = -\left(\frac{\partial\bar{V}}{\partial P}\right)_T \qquad \textbf{[2]}$$

Thus, in principle, by revealing the correlation between K and pressure, the differences in partial molar volume change and compressibility between two conformational states stabilized by two pressures can be determined, leading to important structural information on the molecular volumes of conformers and conformational flexibility. Detailed considerations on the physical meaning and relative scales of $\Delta\bar{V}^0$ and $\Delta\bar{\beta}_T$ have been covered by a recent review.[2]

As discussed at various places, the unfolded or excited states of proteins often possess lower volumes than but are in equilibrium with the ground state.[3, 4] These excited states hold a higher energy and are functionally important (for ligand recognition, for example) yet poorly populated (~ca. 3 %, "invisible" to most spectroscopic techniques) as compared to the ground state (~97 %).[5-8] Thus, high hydrostatic pressure, in principle, not only allows for the determination of the activation volume and compressibility between two conformational states stabilized by two pressures but also offers an avenue to probe these sparsely populated, "invisible", high-energy, and functionally important states by shifting the conformational equilibrium so that the excited states become "visible" to spectroscopic techniques. Revealing the structural basis of the excited states of proteins have led to important findings on protein folding intermediate states, confirmation of known conformational equilibrium, and roles of intermediate states for protein function.[9-11]

Technical advances in high-pressure techniques have been combined with various experimental methods such as Nuclear Magnetic Resonance (NMR) and optical spectroscopy.[3, 4, 9-16] In early-mid 2000s, Hubbell and coworkers began exploring the possibility of high-pressure Electron Paramagnetic Resonance (EPR) in protein science.[1] The immediate challenge was the need of a proper EPR sample holder for Continuous Wave (CW) EPR. The first generation of sample hold was based on folding of a thick borosilica tube with a proper outer diameter (O.D.) to inner diameter (I.D.) ratio (3:1 at least) multiple times, so that sufficient volume of sample can be loaded.[1] The advantage of this approach is that the tubes are EPR silent and low cost. The limitation however, is the fragile portion of the tube at the turns which reduces the reusability of the tube and the maximum pressure that a tube can hold. Then, ceramic high-pressure EPR cells were made commercially available. The high reusability and reliability made them an ideal

substitution for the folded silica tubes, yet the high cost and the intrinsic background signal became a drawback.[2, 17] For double electron-electron resonance (DEER) EPR under high pressure, a sophisticated freezing mechanism had been developed to capture the excited states populated by hydrostatic pressure.[2, 18] Upon overcoming the technical challenges, high-pressure EPR began to be reported in the literature since 2010.

Although EPR does not directly report equilibrium constant, K, or other key parameters (partial molar volume and compressibility), through spectral analysis via simulations, this information can be obtained as well after some theoretical derivations done by Hubbell and coworkers.[1, 2] For example, continuous wave (CW) EPR often reports the correlation time of a spin label sidechain (τ_0), which depends on the internal (τ_i) and protein (τ_P) motions:

$$\frac{1}{\tau_0} = \frac{1}{\tau_i} + \frac{1}{\tau_P} \qquad \textbf{[3]}$$

Each correlation time is further dependent on pressure, P, and the activation volume, $\Delta V^{\ddagger}$:

$$\frac{1}{\tau(P)} = \frac{1}{\tau(0)} e^{\frac{-P\Delta V^{\ddagger}}{RT}} \approx \frac{1}{\tau(0)}\left(1 - \frac{P\Delta V^{\ddagger}}{RT}\right) \qquad \textbf{[4]}$$

Where $\tau(0)$ is the correlation time at 0 bar pressure. Thus,

$$\frac{1}{\tau(P)} = \frac{1}{\tau(0)} - \frac{P}{RT}\left(\frac{\Delta V_i^{\ddagger}}{\tau_i(0)} + \frac{\Delta V_P^{\ddagger}}{\tau_P(0)}\right) \qquad \textbf{[5]}$$

Based the current knowledge of spin label sidechain motion (at 0 bar), or, $\tau_i(0)$, and $\tau_0(0)$ from simulation, $\tau_P(0)$ can be obtained. With some further approximations, one finally obtains

$$\frac{1}{\tau_0(P)} \approx \frac{1}{\tau_0(0)} - \frac{P}{RT}(5 * 10^8 s^{-1})\left(\Delta V_i^{\ddagger} + \Delta V_P^{\ddagger}\right) \qquad \textbf{[6]}$$

Thus, a plot of $1/\tau_0(P)$ versus pressure, P, will result in $\left(\Delta V_i^{\ddagger} + \Delta V_P^{\ddagger}\right)$, with the former term most likely independent of labeled site. The second term is therefore, an indication of protein

conformational flexibility or compressibility at the EPR timescale.[2] Further considerations on distinguishing conformational exchange from rotameric exchange should also be taken into account when analyzing the high pressure CW EPR results. It is also possible to directly probe the intra-protein distance distributions in proteins with two spin labels attached at elevated pressures via DEER EPR. Here, multiple intra-protein distance distributions will directly reflect the conformational flexibility and compressibility of the protein being studied, while a shift in the relative "populations" of certain peaks (as characteristics of certain conformational states) could also directly lead to equilibrium constant, K(P), at elevated pressures, and thus, key thermodynamics parameters such as changes in free energy, activation volumes, and compressibility through Equation 1.

In this review, we will summarize the most recent findings in high-pressure EPR and its applications in protein science, one of the many significant contributions from Prof. Wayne Hubbell in the current Special Issue. We will focus on what each technique can do in protein studies, how to use the technique to measure needed information, and what each measured parameter tells us. We will also discuss the combination of high-pressure EPR with other techniques and the future perspectives of the field.

2. Application of High-Pressure CW EPR

2.1. Measuring compressibility/partial molar volume

For protein sites which do not interact with neighboring residues, the CW EPR spectra often contain a single-component with anisotropic motions. The theoretical basis of the simulation of this kind of spectra is well-established under ambient pressure.[19-23] Typical simulation parameters especially the key order (S) and rate (τ) parameters have been reported in several works.[21-24] Under elevated hydrostatic pressure, the CW EPR spectra were often fit with fixed

S while allowing τ to increase upon pressure increase.[1] A plot of $\ln[\tau/\tau_0]$ vs pressure results in a linear relationship, the slope of which equals $\Delta V^{\ddagger}/RT$, and thus, offers a direct measure of the activation volume, an increase in volume of a solvent cage needed to permit the rotation of the spin label:[1]

$$\ln \frac{\tau(P)}{\tau(0)} = \frac{\Delta V^{\ddagger}}{RT}(P) \qquad [7]$$

Where τ(P) and τ(0) are the rotational correlation times at pressure P and 0. For two well-studied sites, 82R1 and 80R1 (R1 indicates a nitroxide spin labeled sidechain)[25, 26] of a model protein, T4 lysozyme (T4L), at 294 K, the $\Delta V^{\ddagger}$ are 1.2 +/- 0.5 and 2.3 +/- 0.4 mL/mol, respectively, upon analysis of the HP-EPR data (Figure 1). The larger $\Delta V^{\ddagger}$ of 80R1 is likely due to its location at a loop region which offers enhanced backbone motion as compared to 82R1. Unfolding the protein under 8 M urea results in a relatively large, 4.2 +/- 0.5 mL/mol $\Delta V^{\ddagger}$ for 118R, also consistent with the enhanced backbone motion.[1]

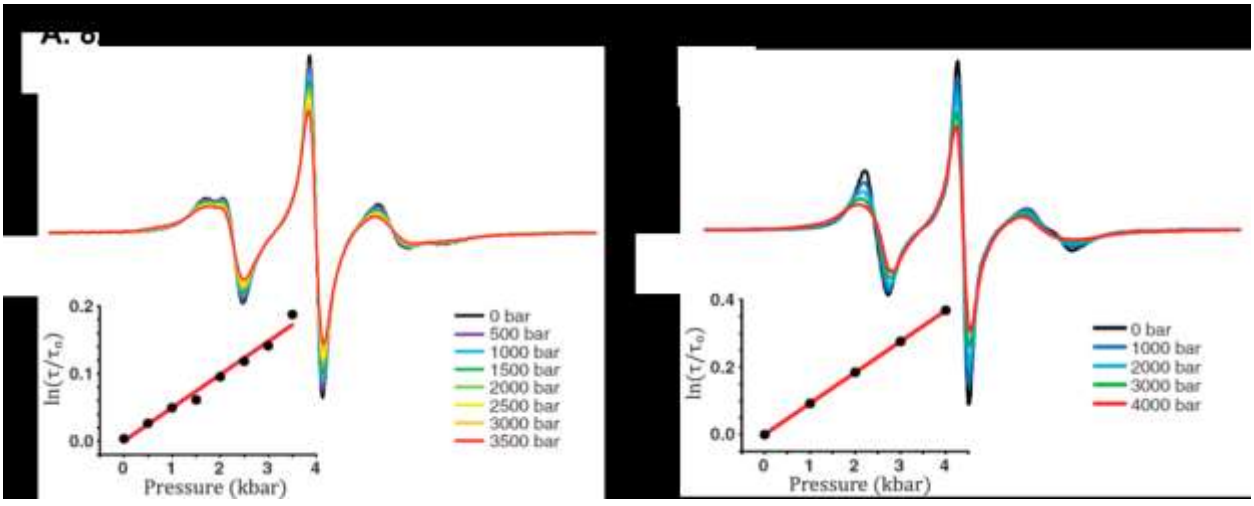

Figure 1. Example HP-EPR data on 82R1 (A) and 80R1(B) for compressibility measurement when the labeled sidechains do not contact neighboring residues. Figure adapted from reference with permission.[1]

For a labeled site in contact with neighboring residues, the activation volume also depends on $\Delta V^{\ddagger}_{i} + \Delta V^{\ddagger}_{p}$, the sum of the internal activation volume of the sidechain and the protein. Thus, knowing $\Delta V^{\ddagger}_{i}$ and the total $\Delta V^{\ddagger}$ can lead to $\Delta V^{\ddagger}_{p}$. For example, in holo-myoglobin (HoloMb),[24] the CW EPR spectra of 22R1 shows very subtle pressure dependence with a $\Delta V^{\ddagger}_{i}$ of 2.27 mL/mol, indicating no interaction with neighboring residues. Using this value, the $\Delta V^{\ddagger}_{p}$ of 42R1, whose CW EPR spectra showed a higher pressure-dependence, was determined to be 7.1 mL/mol using Equation 6.[2, 17] Thus, CW EPR under variable pressure can determine activation volume at a labeled site and report the relative flexibility and compressibility of a protein region.

2.2. Detecting rotameric exchange

For a two-component CW EPR spectrum, typically designated as a "mobile" and an "immobile" component, the contribution could originate from either two conformations of the spin label sidechain (two rotamers) or two protein backbone conformation (but only one rotamer).[23] The difference between the two cases is the isothermal molar compressibility difference (the latter case would be higher). Experimentally distinguishing these two cases have been reported based on osmolytic effects.[23] The equilibrium between the two conformational states can also be perturbed by elevated hydrostatic pressure; plotting ln(K(P)/K(0)) *versus* pressure (K=[m]/[i], [m] and [i] indicate the relative population of the mobile and immobile components, which can be obtained from CW EPR simulation) would result in a linear curve if the two components are due to two rotamers. An example on 44R1 of T4L has been reported to illustrate this point (Figure 2). The fitting gives ΔV^{0} of -9.4 +/- 2.2 mL/mol and $\Delta\beta_{T}$ of 0. The plot of $\ln(\tau/\tau_{0})$ versus pressure for the mobile component resulted in $\Delta V^{\ddagger}$ of 1.7 +/- 0.4 mL/mol, close to other solvent-exposed sites with no interaction with neighboring residues (such as 80R1 and 82R1).

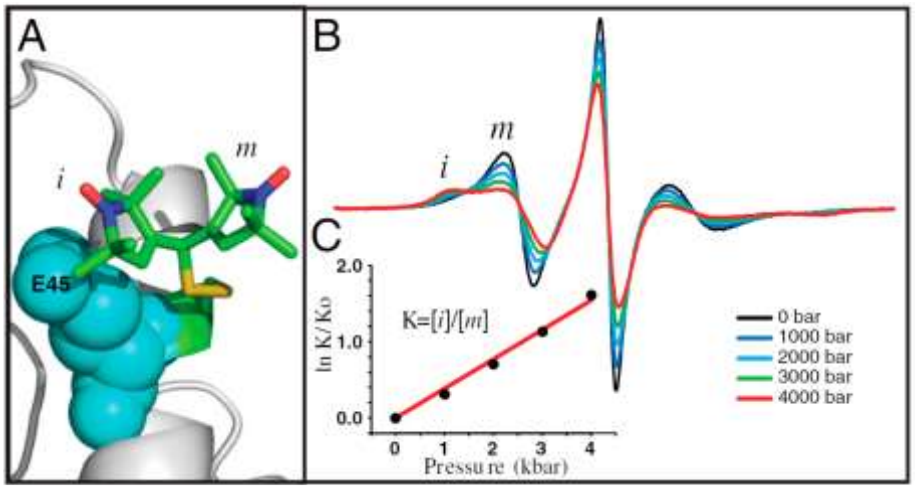

Figure 2. Example data showing HP-EPR on detecting the rotameric exchange on 44R1 of T4L (A). The two-component EPR spectra at elevated pressures (up to 4 kbar; B) can be analyzed. The linear relationship between $\ln(K/K_0)$ over pressure indicates that the two components are originated from two different rotamers of the labeled sidechain. Figure adapted from reference with permission.[1]

2.3. Measuring conformational equilibrium

For a two-component CW EPR spectrum due to two protein conformational states in equilibrium, a plot of $\ln(K(P)/K(0))$ *versus* pressure would result in a non-linear curve. Fitting the curve to Equation 1 will result in ΔV^0 and a non-zero $\Delta\beta_T$. A typical example of conformational equilibria is one of the destabilizing mutants of T4L, 118R1, under 2 M urea. 118R1 is a buried site in T4L, as indicated by the "immobile" CW EPR spectra at varied pressures.[1] Unfolding this site under 8 M urea resulted in sharp spectra due to the unfolding of the whole protein and thus, enhanced backbone motion. Under 2 M urea, however, a two-component CW EPR spectrum was observed under the ambient pressure (Figure 3A), suggesting the equilibrium between partially unfolded and folded states.[1] Then, upon increase in pressure, the lineshape changes accordingly.

A plot of ln(K(P)/K(0)) *versus* pressure resulted in the expected curvature, analysis of which resulted in a ΔV^0 of -51.0 +/- 1.7 mL/mol and $\Delta\beta_T$ of -0.017 +/- 0.001 mL/mol bar. The large ΔV^0 indicates an equilibrium between the native and the unfolded state of 118R1 under 2 M urea.[1]

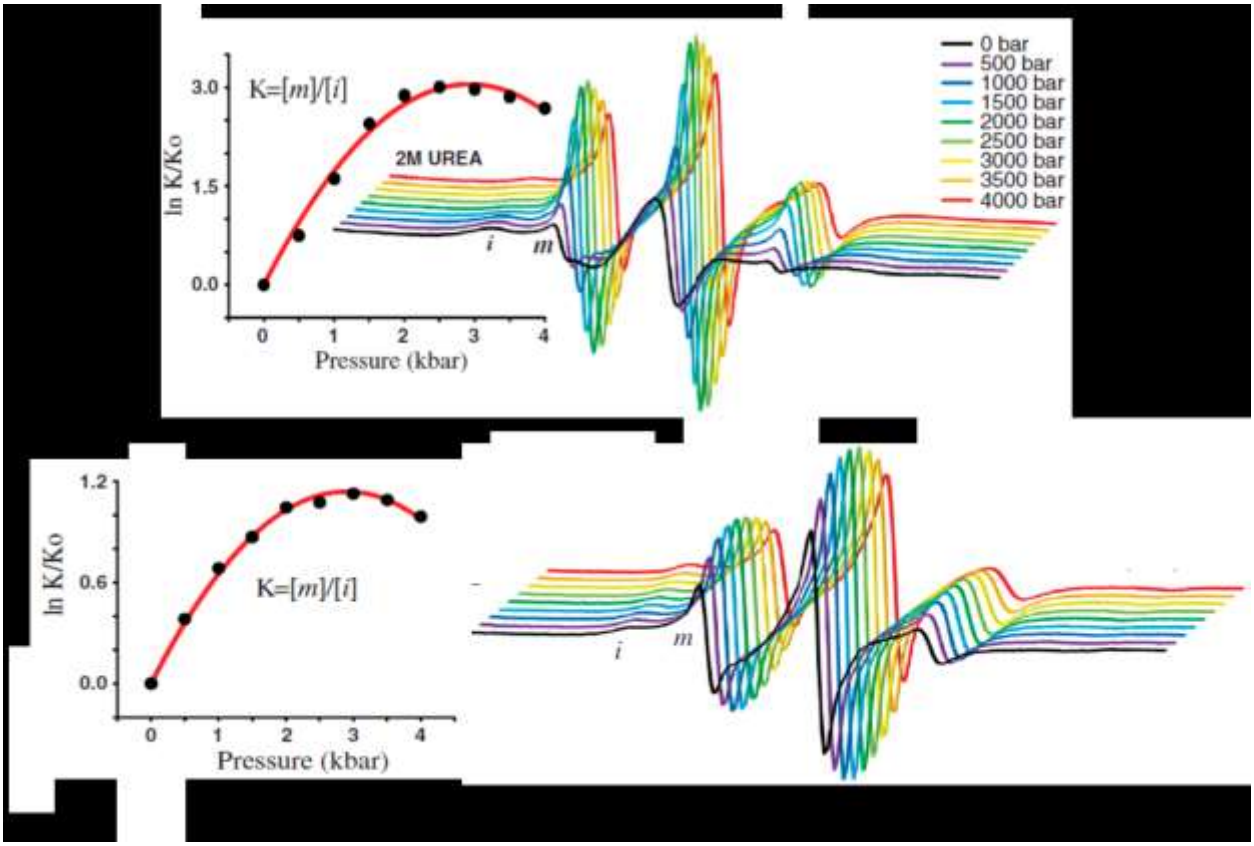

Figure 3. Example HP-EPR data originated from the conformational exchange between two protein conformations at 118R1 (A) and 46R1 (B) as indicated by ln(K/K_0) over pressure. Figure adapted from reference with permission.[1]

Another known site of T4L under conformational equilibrium is 46R1. A plot of ln(K(P)/K(0)) *versus* pressure resulted in a curve as well, analysis of which resulted in a ΔV^0 of -19.2 +/- 0.4 mL/mol and $\Delta\beta_T$ of -0.0066 +/- 0.0002 mL/mol bar (Figure 3B). The relatively small ΔV^0 as compared to the case of 118R1 indicates an equilibrium between the native and an

intermediate state with incomplete unfolding.[1] A more complicated example is the 109R1 of the T4L L99A mutant, a cavity-enlarging mutant. At atmospheric pressure, 109R1 of T4L L99A showed two components with unknown structural origins. Upon pressure increase, a third component consistent with an immobilized state was resolved, suggesting that pressure "populated" an excited state of the T4L L99A mutant. A plot of ln(K(P)/K(0)) *versus* pressure resulted in a curve, analysis of which based on singular value decomposition (SVD) resulted in a ΔV^0 of -57 mL/mol and $\Delta\beta_T$ of 0 mL/mol bar. This ΔV^0 is close to the -56 mL/mol ΔV^0 on the same cavity mutant, T4L L99A, determined by high-pressure fluorescence measurements.[1, 2]

2.4. Sensing protein unfolding by high pressure

In cases where the target protein is partially unfolded (as in the case of T4L 118R1 under 2 M urea), the extent of unfolding can also be quantified via CW EPR spectral simulation which reveals the [m]. High hydrostatic pressure itself may also unfold certain proteins partially as unfolded states of a protein often occupy less hydrostatic volume. Thus, high-pressure CW EPR in combination with SDSL can be directly used to quantify the percentage of protein unfolded at the labeled site by high pressure. Remarkably, such measurement can be carried out in the complex transmembrane environment, demonstrating the power of high-pressure CW EPR in probing otherwise inaccessible biological systems.

A typical example is the high-pressure CW EPR studies on the *E. coli* lipopolysaccharide (LPS) transport protein, LptA, and one of its binding partners, LptC, in the absence and presence of the LPS binding.[27] Under ambient pressure, 3 out of the 4 labeled sites of LptA showed typical linewidth of CW EPR spectra of folded protein in the absence and presence of LPS binding, while one site in a loop showed a typical CW EPR spectrum consistent with fast backbone motion (sharp linewidth). Then, upon increase in pressure, a mobile component characterized by a sharp

lineshape began to be populated at 0.5-1.0 kbar and maximized at ~2.0 kbar.[27] Spectral simulations revealed the relative population of the folded portion of each labeled site in LptA under each pressure, and a decrease in such folded portion over pressure indicated the pressure-induced protein unfolding. LptA unfolds from the N-terminus to the C-terminus while LPS binding did not alter too much of such unfolding behavior. Interestingly, a double mutant of LptA, Q148A/K149A, which stabilize the monomeric state of LptA, seemed to unfold more than the native LptA (often in the oligomeric form) especially at 1.5-2.0 kbar.[27]

On the other hand, LptC was labeled at 5 sites and subjected to the same high-pressure CW EPR studies. Under the ambient pressure, 3 out of the 5 labeled sites showed ordered spectra while the other two showed spectra consistent with rapid motion. Upon pressurization to 2 kbar, only 172R1 of LptC showed a decrease in the folded percentage, 3 sites show the appearance of a new conformation, and one site remained disordered.[27] Thus, LptC seemed to be in a monomeric, folded state under high pressure, which only unfolds its C-terminus. Such influence of pressure on dynamics/folding state changes are likely correlated with functional changes associated with LPS binding and transport.

3. Application of Pressure-Resolved (PR) DEER EPR

3.1. Measuring the scale of compressibility and local conformational flexibility

The name of PR DEER is originated from the fact that, different from high pressure CW EPR conducted in real time under elevated pressure, DEER cannot be carried out on real samples pressurized in real time because the samples need to be frozen to liquid nitrogen temperature at least.[2] Instead, Hubbell and coworkers came up with the brilliant idea to pressurize a DEER sample to the needed pressure, followed by rapid freezing inside of the pressure chamber. Details of the device design, practical operations, and rate of the rapid-freezing are discussed in recent

literature.[2, 5, 18] Once a distance distribution between two labeled protein sites is resolved under elevated pressure, it is possible to evaluate the overall compressibility of the protein of interest and observe the generation of new conformational states populated by pressure.

A typical example is the work done by Hubbell and coworkers on apo- and holo-Mb.[18] In holoMb, 7 pairs of spin labels were created to sense the motion of the core domains of the protein. Under ambient pressure, the distance distributions from all 7 pairs are generally narrow (~3-5 Å), indicating relatively less overall protein flexibility/mobility and thus, high rigidity in protein structure, consistent with the general understanding on holoMb.[24] Upon pressurization to 3 kbar, 5 out of the 7 studied spin pairs showed only a slight broadening in the distance distributions, indicating the low compressibility of holoMb at these regions. The two remaining pairs did exhibit shifts in the nominal distances in distance distribution at 2 kbar (and even additional populations in one of the pairs), indicating the slightly higher compressibility or conformational flexibility in these areas. Overall, however, the distance distributions from PR DEER on most protein regions suggest a relative independence on hydrostatic pressure and incompressibility of the holoMb (Figure 4 left).[18]

The apoMb, on the other hand, showed strong and nonuniform pressure dependence across the protein in PR DEER studies. Under ambient pressure, all 7 labeled pairs showed broadened distance distribution, consistent with the increased conformational flexibility of the apoMb. Upon pressurization, 31R1/70R1 and 70R1/132R1 showed the least pressure dependence and were selected as reference sites located in helices which do not change position under elevated pressure. Helices A, F, D, and G monitored by 12R1, 87R1, 57R1, and 106R1, respectively, in relative to the references displayed broadened distance distribution, which was rationalized to the enhanced conformational flexibility, and new peaks in certain cases, suggesting the formation of new

conformations in these helices (Figure 4 right).[18] Based on these distance constraints, models of the apoMb conformational changes due to pressurization (and the pressure-induced molten globular states of Mb) were constructed.[18] Interestingly, in the same work, the molten globular states induced by pressure (at 2 kbar) and pH (6.0) were compared by PR DEER. Similarities and differences in structural details were found as well, demonstrating the power of PR DEER on probing the structural details of molten globular states of proteins.

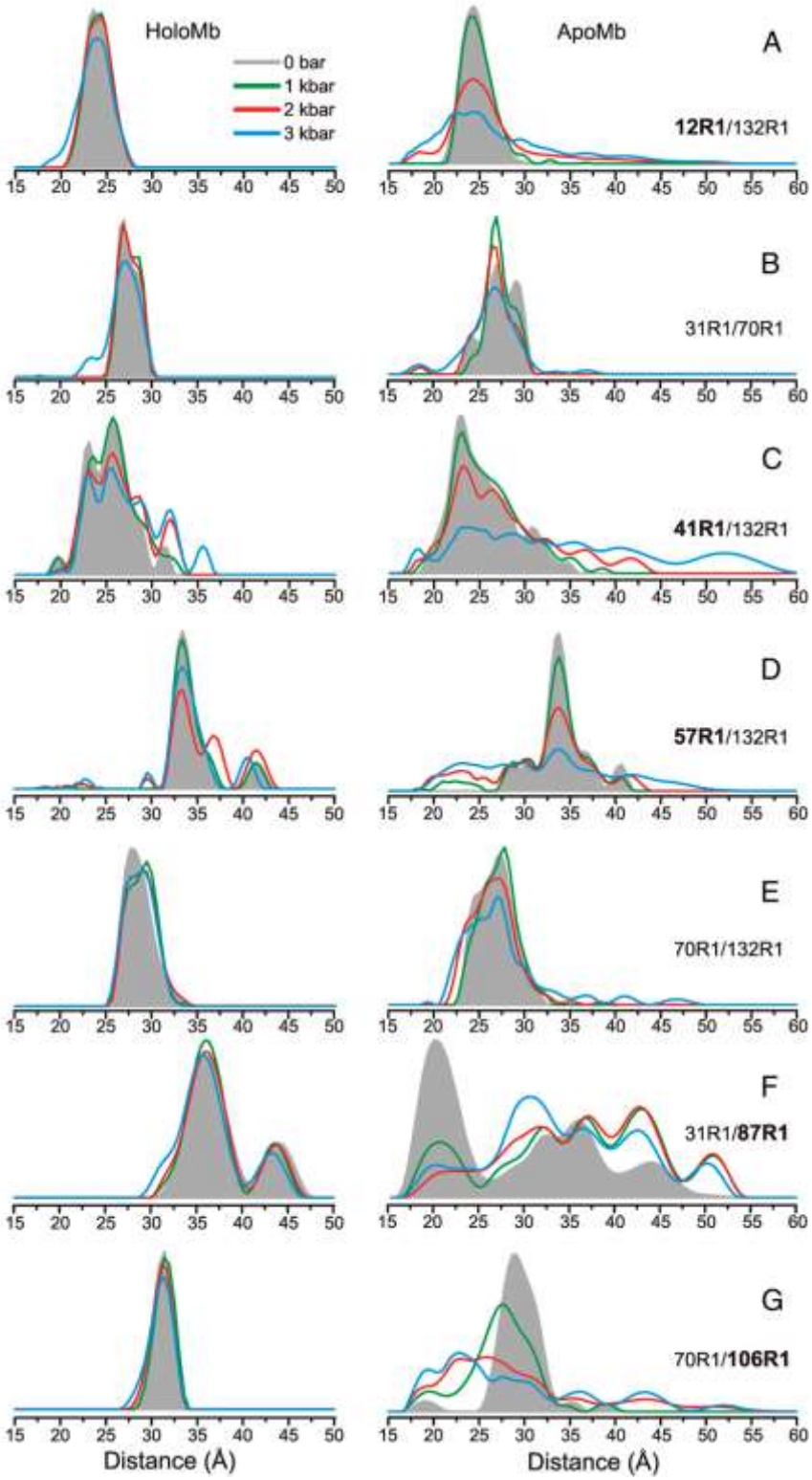
HoloMb
ApoMb
0 bar
1 kbar
2 kbar
3 kbar
A
12R1/132R1
B
31R1/70R1
C
41R1/132R1
D
57R1/132R1
E
70R1/132R1
F
31R1/87R1
G
70R1/106R1
15 20 25 30 35 40 45 50
15 20 25 30 35 40 45 50 55 60
Distance (Å)
Distance (Å)

Figure 4. PR-DEER data on holo- and apo-myoglobin spin labeled at various cysteine pairs across the whole protein (A-G) at 4 different pressures from 0 to 3 kbar. Figure adapted from reference with permission.[18]

3.2. Detecting the structures of low-lying excited states and protein conformational equilibrium

Another intriguing use of PR DEER is to detect and characterize the low-lying, "invisible" excited states of proteins. The underlying principle as discussed above is that pressure increases the relative population of the excited states. Thus, with a proper selection of reference sites in a PR DEER measurement, the increase in the population of a peak in a DEER distance distribution function upon pressurization would indicate the shift in population between the ground state (**G**) and excited states (**E**). The equilibrium between **G** and **E** under varied pressures can also be used to make the plot of ln(K(P)/K(0)) *versus* pressure, fitting of which will result in the ΔV^0 and the free Gibbs energy change, $\Delta G_{\mathbf{G}\leftrightarrow\mathbf{E}}$.

A typical example is a study by Hubbell and coworkers on a series of cavity-forming mutants of T4L, L99A, L99A/G113A, and L99A/G113A/R119P.[5] The volumes of the cavity formed via these mutations are different, and a conformational equilibrium between the **G** and **E** states of each mutant was known in the literature via other techniques. In PR DEER studies carried out by Hubbell's team, the distance distribution between a few spin-labeled residue pairs in the L99A mutant (for example 109R1/140R1 and 89R1/109R1) changed only slightly upon elevated pressure (to 4 kbar).[5] The peak in the distance distribution consistent with the **E** state was not highly populated, consistent with the literature.[16] A rationalization was that the energy of the **E** state was so high that an equilibrium between the **G** and **E** states cannot be observed at the

experimental conditions. Instead, a hydrated **G** state, namely $\mathbf{G_H}$, was observed instead, which was more likely due to the structural fluctuation within the **G** state especially at 0-2 kbar, possibly resulting from the hydration of the L99A cavity (as compared to filling in the cavity with a sidechain; see below).

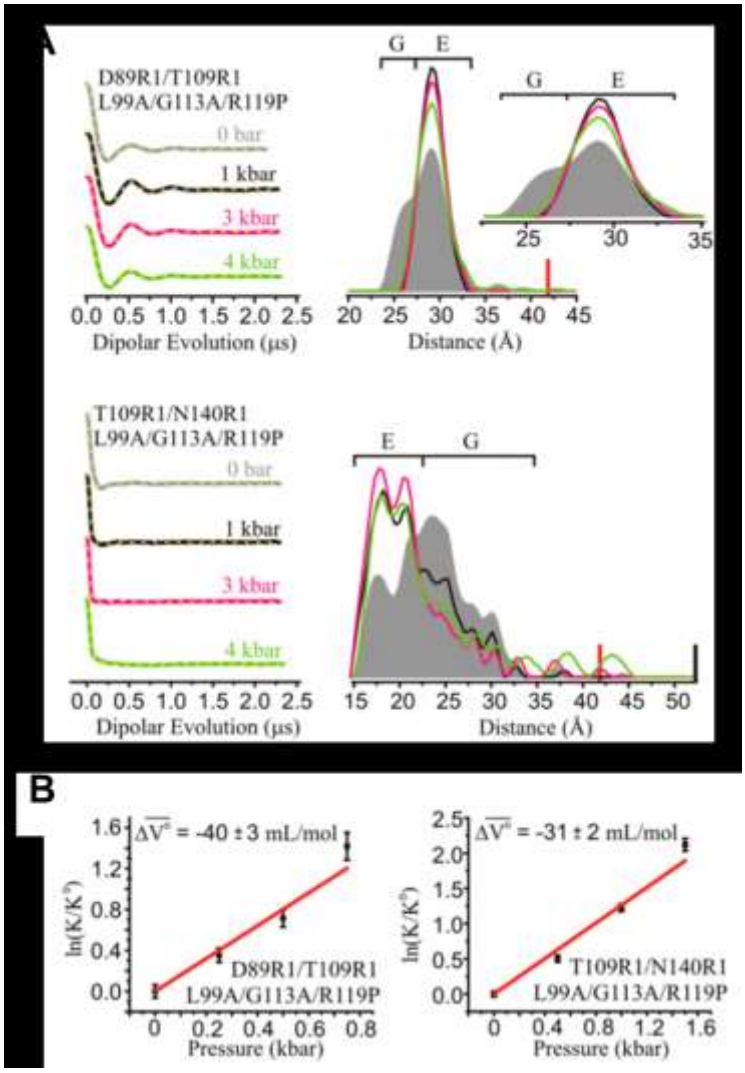

Figure 5. Representative PR-DEER data on one of the T4L cavity mutants, L99A/G113A/R119P between two pairs of labeled sites (89R1/109R1 and 109R1/140R) at 4 different pressures (A). The distance distribution can be utilized to extract the populations of the ground and excited

states, a plot of which over pressure results in the activation volumes. Figure adapted from reference with permission.[5]

In L99A/G113A, and L99A/G113A/R119P, the energy of the **E** state is lowered so that an equilibrium can be easily observed. PR DEER studies on various pairs of spin labeled residues (for example 72R1/109R1, 89R1/109R1, and 109R1/140R1; Figure 5A) in these mutants showed a gradual increased in the intensity of the peak in the distance distribution corresponding to the **E** state as the pressure was increased gradually. The measured distance distribution changes, especially the distance between 109R1 and the reference sites (72R1, 89R1, and 140R1; PR DEER show that the distance distributions among these sites were not significantly affected by pressure), were fit via multi-modal Gaussian functions, which resulted in the relative population of the **G** and **E** states (both were characterized without pressurization before PR DEER measurements) and thus, the equilibrium constant at each pressure for each pair. Plotting ln(K(P)/K(0)) as a function of pressure then resulted in the ΔV^0 on the order of -29 to -40 mL/mol (Figure 5B).[5] This volume is close to the volume of Phe114 (F114), an interesting finding suggesting that F114 sidechain was moved to fill in the cavity. Such a movement was also confirmed by distance triangulation using the nominal distances of each peak (**G** or **E** state). Such a structure-relaxation mechanism is the first direct experimental observation of volume reduction by pressure as opposed to the hydration of the cavity with water.[5]

Another elegant application of the PR DEER EPR is to reveal rare conformations of a G protein coupled receptor (GPCR), the β_2 adrenergic receptor (β_2AR).[28] β_2AR is known to be sensitive to agonist and inverse agonist binding, which shift its conformation by a large-scale movement of the transmembrane helix 6 (TM6). Spin labels on TM4 (as a reference) and TM6

were then shown to confirm such as movement upon binding of epinephrine (epi, agonist), ICI-118,551 (inverse agonist), and epi/G protein mimic (Nb80) under the atmospheric pressure, wherein peaks at 33 and 40.4 Å are rationalized to the inactive state and that at 48.7 Å the active state of the β_2AR. Upon pressurization to 4.0 kbar, the population of the active state-peak was increased to 73% (and the change was completely reversible).[28] Plotting ln(K(P)/K(0)) *versus* pressure resulted in ΔG^0 of 3.1 +/-0.2 kcal/mol (meaning 0.5% of the unliganded receptors were in an active conformation under ambient conditions), ΔV^0 of -62 +/-8 mL/mol, and $\Delta\beta_T$ of -0.012+/-0.003 mL/mol bar.[28] The distance distribution changes upon pressurization was also found to be ligand dependent. This work demonstrated the use SDSL and PR DEER EPR to reveal rare conformations of β_2AR, a membrane protein.

4. Combining with Other High-Pressure Techniques

When combining high pressure EPR studies (and the unique structural and dynamic information of the target proteins) with other high-pressure techniques such as CD and fluorescence, more in-depth and/or complete structural information can be obtained. A typical example is the combination of high-pressure CD and CW EPR for the study of holoMb and apoMb between 0 and 2.0 kbar at pH 6.0 and 4.1.[17] Here high-pressure CD reported the ellipticity and the secondary structure content at different pressures (0-2 kbar with a 0.5 kbar interval), which also resulted in ΔG^0 and ΔV^0 for holoMb and apoMb at pH 4.1. Then, high pressure CW EPR on one representative residue of each helix of Mb reported site-specific pressure responses under the same pH conditions. Being able to obtain both global and local structural information under elevated pressure allowed Hubbell and coworkers to obtain in-depth understanding of Mb. In particular, at pH 6, the helix percentage of the high-pressure excited state of apoMb is similar to that of apoMb at 0 bar; EPR revealed a slow structural fluctuation slowly on the EPR time scale.

At pH 6, the molten globule of apoMb stabilized by high pressure is different from the well-known apoMb stabilized at pH 4.1 (ambient pressure). At pH 4.1, the pressure-populated states of holoMb and apoMb possess a lower helical content.[17] When combining the findings from high pressure CD with those from PR DEER, one can conclude that Mb possesses nm scale rigid body motion of helices in the molten globule state.[18]

Another contribution by Hubbell and coworkers is to combine high pressure fluorescence with high pressure CW EPR to probe the conformational mobility in cytochrome P450 3A4.[29] Although the two techniques probe different physical parameters of the target protein, the effect of pressure on cytochrome P450 3A4 should be independent of the chosen experimental technique. Bearing this in mind, principal component analysis (PCA) was combined with target factor analysis (TFA) to simultaneously analyze the data from high pressure fluorescence and CW EPR when a fluorescence and EPR label was attached to the same site of cytochrome P450 3A4 (C85 and C409 for example) in the absence and presence of an effector (testosterone, or, TST). The results revealed a TST-dependent conformational equilibrium between the open and closed states of CYP3A4.[29] Finally, high pressure CD, CW EPR, and PR DEER were combined to offer a comprehensive study of the cavity mutants of T4L (discussions see above).[5]

5. Conclusion and Future Perspectives

High pressure EPR alone or in combination with other high pressure techniques will open a new avenue to probe important structural information in proteins and lead to otherwise inaccessible conclusions. Prof. Hubbell and coworkers have completed key instrumentation development and established foundations of theories as demonstrated in various cases, from globular proteins to transmembrane proteins. There is no doubt that high pressure EPR will continue making significant contributions to protein science. Potential improvement needed for

broader application of high pressure EPR could be focused on making the high pressure CW or pressure-solved DEER EPR measurement more accessible to a general protein science/biophysics research laboratory, via simpler setup and experimental procedures, for example. The freezing rate should be enhanced while the freezing temperature should be decreased in the PR DEER EPR setup so that a lower temperature could be reached in a shorter timeframe. Or, unique spin labels or strategies to "capture" the conformational states populated by high pressure can be applied so that no freezing is needed in high pressure DEER measurements.[30, 31] Lastly, of course, more biological systems should be studied by high pressure EPR, which will with no doubt lead to important discoveries in protein science.

Acknowledgements

This work is supported by the National Science Foundation (NSF MCB 1942596 and NSF CBET 2217474 to Z. Y.).

Declarations

Ethical Approval

Not applicable.

Competing interests

The authors claim no competing interests.

Authors' contributions

A. M., Z. A., and Z. Y. wrote the main manuscript text and prepared figures. M.L. and Q.L. assisted in literature search and figure preparation. A. F. and M. W. L. F., and W. S. assisted in literature search and writing. All authors reviewed the manuscript.

Funding

This work is supported by the National Science Foundation (NSF MCB 1942596 and NSF CBET 2217474).

Availability of data and materials

Not applicable.

References

[1] J. McCoy, W.L. Hubbell, High-pressure EPR reveals conformational equilibria and volumetric properties of spin-labeled proteins. Proc. Natl. Acad. Sci. **108,** 1331-1336 (2011)
[2] M.T. Lerch, Z. Yang, C. Altenbach, W.L. Hubbell, Chapter Two - High-Pressure EPR and Site-Directed Spin Labeling for Mapping Molecular Flexibility in Proteins, in: P.Z. Qin, K. Warncke (Eds.) Methods in Enzymology, Academic Press2015, pp. 29-57.
[3] H. Li, K. Akasaka, Conformational fluctuations of proteins revealed by variable pressure NMR. Biochim. Biophys. Acta Prot. Proteom. **1764,** 331-345 (2006)
[4] K. Akasaka, Probing Conformational fluctuation of proteins by pressure perturbation. Chem. Rev. **106**, 1814-1835 (2006)
[5] M.T. Lerch, C.J. López, Z. Yang, M.J. Kreitman, J. Horwitz, W.L. Hubbell, Structure-relaxation mechanism for the response of T4 lysozyme cavity mutants to hydrostatic pressure. Proc. Natl. Acad. Sci. **112**, E2437-E2446 (2015)
[6] G. Bouvignies, P. Vallurupalli, D.F. Hansen, B.E. Correia, O. Lange, A. Bah, R.M. Vernon, F.W. Dahlquist, D. Baker, L.E. Kay, Solution structure of a minor and transiently formed state of a T4 lysozyme mutant. Nature **477**, 111-114 (2011)
[7] A.E. Eriksson, W.A. Baase, X.J. Zhang, D.W. Heinz, M. Blaber, E.P. Baldwin, B.W. Matthews, Response of a protein structure to cavity-creating mutations and its relation to the hydrophobic effect. Science **255**, 178-183 (1992)
[8] F.A.A. Mulder, A. Mittermaier, B. Hon, F.W. Dahlquist, L.E. Kay, Studying excited states of proteins by NMR spectroscopy. Nat. Struct. Biol. **8**, 932-935(2001)
[9] K. Kuwata, H. Li, H. Yamada, C.A. Batt, Y. Goto, K. Akasaka, High pressure NMR reveals a variety of fluctuating conformers in β-lactoglobulin. J. Mol. Biol. **305,** 1073-1083 (2001)
[10] R. Kitahara, S. Yokoyama, K. Akasaka, NMR snapshots of a fluctuating protein structure: ubiquitin at 30bar–3kbar. J. Mol. Biol. **347**, 277-285 (2005)
[11] R. Kitahara, S. Sareth, H. Yamada, E. Ohmae, K. Gekko, K. Akasaka, High pressure NMR reveals active-site hinge motion of folate-bound escherichia coli dihydrofolate reductase. Biochemistry **39**, 12789-12795 (2000)
[12] R. Kitahara, H. Yamada, K. Akasaka, P.E. Wright, High pressure NMR reveals that apomyoglobin is an equilibrium mixture from the native to the unfolded. J. Mol. Biol. **320**, 311-319 (2002)
[13] R. Winter, J. Jonas, High Pressure Molecular Science, SpringerLink1999.
[14] R.W. Peterson, A.J. Wand, Self-contained high-pressure cell, apparatus, and procedure for the preparation of encapsulated proteins dissolved in low viscosity fluids for nuclear magnetic resonance spectroscopy. Rev. Sci. Instr. **76**, 094101 (2005)
[15] Y. Fu, V. Kasinath, V.R. Moorman, N.V. Nucci, V.J. Hilser, A.J. Wand, Coupled motion in proteins revealed by pressure perturbation. J. Am. Chem. Soc. **134**, 8543-8550 (2012)
[16] N.V. Nucci, B. Fuglestad, E.A. Athanasoula, A.J. Wand, Role of cavities and hydration in the pressure unfolding of T4 lysozyme. Proc. Natl. Acad. Sci. **111,** 13846-13851 (2014)
[17] M.T. Lerch, J. Horwitz, J. McCoy, W.L. Hubbell, Circular dichroism and site-directed spin labeling reveal structural and dynamical features of high-pressure states of myoglobin. Proc. Natl. Acad. Sci. **110**, E4714-E4722 (2013)
[18] M.T. Lerch, Z. Yang, E.K. Brooks, W.L. Hubbell, Mapping protein conformational heterogeneity under pressure with site-directed spin labeling and double electron-electron resonance. Proc. Natl. Acad. Sci. **111,** E1201-E1210 (2014)

[19] D.E. Budil, S. Lee, S. Saxena, J.H. Freed, Nonlinear-least-squares analysis of slow-motion EPR spectra in one and two dimensions using a modified levenberg-marquardt algorithm. J. Magn. Reson. A **120**, 155-189 (1996)
[20] S. Stoll, A. Schweiger, EasySpin, a comprehensive software package for spectral simulation and analysis in EPR. J. Magn. Reson. **178,** 42-55 (2006)
[21] A. Gross, L. Columbus, K. Hideg, C. Altenbach, W.L. Hubbell, Structure of the KcsA potassium channel from streptomyces lividans: a site-directed spin labeling study of the second transmembrane segment. Biochemistry **38**, 10324-10335 (1999)
[22] L. Columbus, T. Kálai, J. Jekö, K. Hideg, W.L. Hubbell, Molecular motion of spin labeled side chains in α-helices: analysis by variation of side chain structure. Biochemistry **40**, 3828-3846 (2001)
[23] C.J. López, M.R. Fleissner, Z. Guo, A.K. Kusnetzow, W.L. Hubbell, Osmolyte perturbation reveals conformational equilibria in spin-labeled proteins. Prot. Sci. **18**, 1637-1652 (2009)
[24] C.J. López, S. Oga, W.L. Hubbell, Mapping molecular flexibility of proteins with site-directed spin labeling: a case study of myoglobin. Biochemistry, **51**, 6568-6583 (2012)
[25] A.P. Todd, J. Cong, F. Levinthal, C. Levinthal, W.L. Hubbell, Site-directed mutagenesis of colicin E1 provides specific attachment sites for spin labels whose spectra are sensitive to local conformation. Prot. Struct. Funct. Bioinform. **6,** 294-305 (1989)
[26] M.R. Fleissner, M.D. Bridges, E.K. Brooks, D. Cascio, T. Kálai, K. Hideg, W.L. Hubbell, Structure and dynamics of a conformationally constrained nitroxide side chain and applications in EPR spectroscopy. Proc. Natl. Acad. Sci. **108**, 16241-16246 (2011)
[27] K.M. Schultz, C.S. Klug, High-pressure EPR spectroscopy studies of the E. Coli lipopolysaccharide transport proteins LptA and LptC. Appl. Magn. Reson. **48**, 1341-1353 (2017)
[28] M.T. Lerch, R.A. Matt, M. Masureel, M. Elgeti, K.K. Kumar, D. Hilger, B. Foys, B.K. Kobilka, W.L. Hubbell, Viewing rare conformations of the β2 adrenergic receptor with pressure-resolved DEER spectroscopy. Proc. Natl. Acad. Sci. **117**, 31824 (2020)
[29] Dmitri R. Davydov, Z. Yang, N. Davydova, James R. Halpert, Wayne L. Hubbell, Conformational mobility in cytochrome P450 3A4 explored by pressure-perturbation EPR spectroscopy. Biophys. J. **110**, 1485-1498 (2016)
[30] Z. Yang, Y. Liu, P. Borbat, J.L. Zweier, J.H. Freed, W.L. Hubbell, Pulsed ESR dipolar spectroscopy for distance measurements in immobilized spin labeled proteins in liquid solution. J. Am. Chem. Soc. **134**, 9950-9952 (2012)
[31] Z. Yang, G. Jiménez-Osés, C.J. López, M.D. Bridges, K.N. Houk, W.L. Hubbell, Long-range distance measurements in proteins at physiological temperatures using saturation recovery EPR spectroscopy. J. Am. Chem. Soc. **136**, 15356-15365 (2014)